Mansoura Engineering Journal

Volume 39 | Issue 1 Article 6

7-15-2020

Experimental Investigation of Natural Convection Heat Transfer through Rectangular Enclosure Filled with TiO2-Water Nanofluid.

Amro Abou Elenein
Researcher at Mechanical Power Engineering Department., Faculty of Engineering., Mansoura.

Ahmed Sultan
Professor of Mechanical Power Engineering Department., Faculty of Engineering., El-Mansoura University., Mansoura., Egypt.

Hesham Mostafa
Mechanical Power Engineering Department., Higher Technological Institute., Tenth of Ramadan City., Egypt., dr.heshammostafa@yahoo.com

Ahmed Hegazi
Associate Professor., Mechanical Engineering Department., El-Mansoura University., CO 35516., Egypt., ahmedabd_elsallam@yahoo.com

Recommended Citation

Abou Elenein, Amro; Sultan, Ahmed; Mostafa, Hesham; and Hegazi, Ahmed (2020) "Experimental Investigation of Natural Convection Heat Transfer through Rectangular Enclosure Filled with TiO2-Water Nanofluid.," *Mansoura Engineering Journal*: Vol. 39 : Iss. 1 , Article 6.
Available at: https://doi.org/10.21608/bfemu.2020.103097

Experimental Investigation of Natural Convection Heat Transfer Through Rectangular Enclosure Filled with TiO_2-Water Nanofluid

دراسة عملية لإنتقال الحرارة بالحمل الحر خلال كهف مستطيل مملؤ بمائع النانو ـ أكسيد التيتانيوم- ماء

Amro M. Abou Elenein *, Ahmed A. Sultan *, Hesham M. Mostafa ** and Ahmed A. Hegazi *.

***Egypt Mansoura, Mansoura University, Mech. Power Eng. Dept .**

**** Egypt, Tenth of Ramadan City, Higher Technological Institute, Mech. Power Eng. Dept.**

ملخص البحث

فى هذا البحث تم عمل دراسة عملية لإنتقال الحرارة بالحمل الحر خلال كهف مستطيل مملؤ بمائع النانو- أكسيد التيتانيوم- ماء. تم إستخدام كهفين بنسبه باعيه بين العرض إلى الإرتفاع تساوى 1, 2 وأيضاً عدد رايلى يتراوح مابين10^5 إلى 10^9. السطح السفلى للكهف يتم تسخينه بفيض حرارى ثابت يتراوح مابين 40 إلى 6600 وات/م^2 ويتم تبريد الجدار العلوى بتيار هوائى والجدران الجانبيه معزوله. تم مقارنة نتائج إنتقال الحرارة بنتائج إنتقال الحرارة من الأبحاث السابقة وذلك للوقوف على مدى التقارب بينهما. أوضحت النتائج أن معدل إنتقال الحرارة يكون فى حالة النسبة الباعيه تساوى 2 أعلى منها فى حالة النسبه تساوى1. متوسط درجة حرارة السطح الساخن تقل مع زيادة التركيز الحجمى لجسيمات النانو حتى 0.8 % ثم تزيد مع زيادة التركيز الحجمى لجسيمات النانو. متوسط درجة حرارة السطح الساخن يزيد مع زيادة عدد رايلى .معدل إنتقال الحرارة يزيد مع زيادة عدد رايلى حتى 10^8 ثم يقل مع زيادة عدد رايلى وتكون أعلى قيمة لة عند التركيز الحجمى لجسيمات النانو يساوى 0.8% وأيضاً تم الحصول على معادلة بين إنتقال الحرارة و عدد رايلى و التركيز الحجمى لجسيمات النانو.

ABSTRACT

Experimental investigations on natural convection heat transfer have been carried out inside rectangular enclosures filled with TiO_2- water nanofluid. Two enclosures are used with two different aspect ratios of 1 and 2 and the modified Rayleigh number based on the enclosure height in the range $10^5 \prec \mathrm{Ra}^* \prec 10^9$. The bottom surface of the enclosure is heated using a constant heat flux in the range from 40 to 6600 W/m^2 while the upper surface is cooled by forced air stream, and side walls are insulated. The heat transfer rate for aspect ratio, AR=2, is higher than that for the aspect ratio A= 1. The average temperature of hot surface decreases with the increase of nanoparticles volume concentration, ϕ, up to minimum values at ϕ=0.8 % and then increases with further increase in ϕ. The average hot surface temperature increases with the increase in the modified Rayleigh number. The heat transfer rate increases with the increase of the modified Rayleigh number up to maximum values of about $Ra^* = 10^8$ and then decreases with further increase in Ra^*. The highest value of the average Nusselt number is located at ϕ = 0.8%. A general correlation is obtained for calculating the average heat transfer rate as a function of modified Rayleigh number and nanoparticles volume concentration.

Key words: Heat transfer, Rectangular enclosure, Experimental analyses, TiO_2– water nanofluid.

1. INTRODUCTION

Air-cooling is one of the preferred methods for cooling computer and other electronic equipment due to its simplicity and low cost. The electronic components are treated as heat sources embedded on flat surfaces [1]. In many applications natural convection is the only feasible mode of cooling of the heat source. There are numerous other practical applications of natural convective cooling in rectangular enclosures with various combinations of the temperature gradients, cavity aspect ratios, placement of the heat source and cold surfaces, etc. A comprehensive review of such enclosures has been reported by Ostrach [2]. Natural convection cooling of a localised heat source at the bottom of a nanofluid-filled enclosure was numerically investigated by Aminossadati and Ghasemi [3]. Natural convection heat transfer inside vertical circular enclosure filled with water-based Al_2O_3 nanofluids was experimentally investigated by Ali et al. [4]. The aim of the present paper is to investigate natural convection in rectangular enclosures heated from below with various heat fluxes in the range from 40 to 6600 W/m^2 and cooled from above with insulated side walls. The study is conducted experimentally for width-to-height aspect ratio of the enclosure of 1 and 2, and the modified Rayleigh number based on the enclosure height in the range $10^5 \prec \mathrm{Ra}^* \prec 10^9$. The temperature distributions and heat transfer rates are analyzed and discussed for TiO_2 – water nanofluid filled.

Nomenclature

A_H	area of hot surface (m^2)
A	aspect ratio, (L/H)
C_p	specific heat at constant pressure ($J/(kg \times K)$)
g	gravitational acceleration (m/s^2)
H	height of the enclosure (m)
h	convective heat transfer coefficient ($W/m^2 K$)
I	current (Ampere)
k	thermal conductivity ($W/m\ K$)
L	width of the enclosure (m)
Nu	Nusselt number, (hH/k_{nf})
P	pressure (Pa)
Q_{Bh}	heat lost from the bottom wall in contact with the electric heater (W)
Q_{cv}	convective heat transfer (W)
q''_{cv}	convective heat flux, (Q_{cv}/A_H) (W/m^2)
Q_{rad}	heat lost from the enclosure by radiation heat transfer (W)
Q_{si}	heat lost through the insulated side walls (W)
Q_{total}	electrical input power (W)
Ra^*	modified Rayleigh number based on the enclosure height, ($g\beta_{nf} Q_{cv} H^4/(A_H \nu_{nf}\ k_{nf}\ \alpha_{nf})$)
R	thermal resistance (W/K)
T	temperature (K)
V	voltge (volt)
x, y	dimensional coordinates (m)

Greek Symbols

α	thermal diffusivity (m^2/s)
β	coefficient of volumetric thermal expansion (K^{-1})
δ_{ins}	insulation thickness (m)

ΔX	thickness of the copper plate (m)
ν	kinematic viscosity, (μ/ρ) (m^2/s)
ϕ	nanoparticles volume concentration (%)
μ	dynamic viscosity $(kg/(m\times s))$
ρ	density (kg/m^3)

Subcripts

Bh	below heater
C	cold
cv	convection
H	hot
ins	insulation
f	fluid
nf	nanofluid
o	outside
P	particle
si	sides of the enclosure
∞	ambient

Superscripts

-	average quantity

2. EXPERIMENTAL APPARATUS

The considered physical model is shown in Fig. (1). It consists of a rectangular enclosure of dimension (L × H) and depth (L), whose upper wall is kept at a cold constant temperature, T_C. The aspect ratio of the enclosure is defined as A = L/H. The bottom wall has an embedded symmetrical heat source with constant heat flux, q''_{cv}. Side walls are insulated by glass wool insulation of 50 mm thickness from Kimmco company. The experimental apparatus is shown in Fig. (2). As seen from this figure, the rectangular enclosure (7) is made of copper ($k = 401 W/m.K$ [5]) with height of 0.05 m and with two different aspect ratios (1, and 2). The enclosure is heated using an electric heater (8) with a wire diameter of 0.43 mm. The electric heater is electrically insulated by a mica sheet (6) (0.33 mm thickness) and a thermal insulation of glass wool (9) ($k = 0.046 W/m.K$ [5]). Figure (2) also shows two connections on the sides of the enclosure: one connection (17) for filling the enclosure via tank (16) and charging valve (V1) and the other connection (20) for fluid drain via outlet valve (V3). Connection (18) is used for enclosure evacuation from air or old fluid using vacuum pump (19) via valve V2. The surface temperature (T) is measured at sixteen points along the surface of the enclosure by using thermocouples type K (0.5 mm tip diameter). The thermocouples are connected to computer (11) via temperature recorder (12). The temperature recorder used in the present study is supplied by the Pico Technology, made in UK with accuracy ± 0.5 ^{o}C and conversion time 100 ms. As shown in Fig. (2), five thermocouples at the bottom copper surface (hot surface) and similar five thermocouples are glued at the top copper surface (cold surface). In order to calculate the heat lost away from the heater, two thermocouples are distributed on the top and bottom of the glass wool (9) located at the lower surface of the electric heater (8) as seen in Fig. (2). Three thermocouples are distributed on the outer surfaces of the enclosure (side surfaces) and one on the outside surfaces of the insulation to measure the heat lost from the side surfaces and measuring the temperature distribution at these surfaces. All thermocouples are connected to a 16-channels data acquisition system, which are connected to a computer where the measured

temperatures are stored for further analysis. It should be mentioned that the cold surface is subjected to an air stream of 1.6 m/s air velocity flowing from inlet section (15) to outlet section (13) by using a fan (14) to cool the upper surface. It is worth mentioning that the power, dissipated from the heater, is measured by a voltameter (3) and ammeter (4). Enclosure internal pressure is measured by a pressure gage (P1) for vacuum pressure and (P2) for high pressure via valves. Heat transfer data are generated by controlling the input power to the heater via the variac (2) in order to ensure that the maximum hot plate surface temperature does not exceed $90^{o}C$ as given by Huang et al. [6], recommended for electronic equipment cooling systems.

3. PREPARATION OF TIO_2-WATER NANOFLUID

The Titanium Oxide-water nanofluid (water based TiO_2) is used in the present study. Titanium Oxide is supplied by the Sigma-Aldrich. In order to characterize the size of the particles, a sample of the diluted dispersed suspension is dried and grinded into fine particles. Figure (3) shows the imaging using a Scanning Electronic Microscope (JEOL-JEM-1011). As seen in this figure the minimum size is around 76.99 nm and some are agglomerated to bigger sizes. The concentrated nanofluid provided 2% was diluted to 1.8%, 1.6%, 1.4%, 1.2%, 1%, 0.8%, 0.6%, 0.4% and 0.2 % by volume using distilled water. These new diluted solutions are ultrasonically vibrated to insure complete dispersions of the nanoparticles and to be sure that agglomerations seen in Fig. (3) are broken to some extent into nanometer range [7]. The stability of the nanofluid samples is checked by taking a photo of the sample just after the ultrasonic vibration and two days later where no precipitation is observed in those two days period. The thermo-physical properties of the nanoparticle are given in Table (1) [8].

	ρ	C_p	K	β
Titanium Oxide (TiO_2)	4250	686.2	8.9538	0.9

Table (1) Thermo-physical properties nanoparticle [8].

4. Data Reduction

The heat generated by the heater is dissipated through the copper hot plate and then to the fluid medium by convection. The heat flux q''_{cv} is calculated by dividing the consumed power (after deducting the heat lost from the back side of the heater and from the enclosure sides by conduction and radiation) by the surface area A_H. Total electrical power Q_{total} input to heater is given by:

$$Q_{total} = I \times V \quad (1)$$

Where, I, and V are the current, and voltage, respectively. The heat transfer by convection Q_{cv} through the fluid in the vertical direction is given by:

$$Q_{cv} = Q_{total} - Q_{si} - Q_{Bh} - Q_{rad} \quad (2)$$

Where: Q_{si} is the heat lost through the side walls and calculated by:

$$Q_{si} = A_{ins,si}\, k_{ins} (\bar{T}_{nf} - \bar{T}_{o,si}) / \delta_{ins,si} \quad (3)$$

The heat lost from the bottom wall in contact with the electric heater Q_{Bh} is calculated by:

$$Q_{Bh} = A_{ins,Bh}\, k_{ins} (\bar{T}_{H} - \bar{T}_{o,Bh}) / \delta_{ins,Bh} \quad (4)$$

The heat flux density q''_{cv} is given by:

$$q''_{cv} = Q_{cv} / A_H \quad (5)$$

Where, $A_{ins,Bh}$, $A_{ins,si}$, A_H, and k_{ins} are the surface area of the insulation below the electric heater, the surface area of the side walls, the surface area of hot surface and the thermal conductivity of the insulation,

respectively. $\delta_{ins,Bh}$, and $\delta_{ins,si}$ are the insulation thickness below the electric heater and the insulation thickness at side walls, respectively.

It should be noted that, all physical properties of the nanofluid are evaluated at the mean temperature of the nanofluid $\bar{T}_{nf} = (\bar{T}_H + \bar{T}_C)/2$. Where, $\bar{T}_C$, $\bar{T}_H$, $\bar{T}_{o,si}$, and $\bar{T}_{o,Bh}$ are the average surface temperatures of the cold side, hot side, outside of side walls and outside below the electric heater, respectively. It should be mentioned that the radiation heat transfer Q_{rad} is neglected since the fluid is liquid with a maximum temperature of 90 ^oC. Measurements show that, the fraction of heat lost by conduction through the insulation below the heater and from the side walls are 1.1% and 0.7 % respectively at most cases.

The average surface temperature is used to calculate the average heat transfer coefficient $\bar{h}$ at each convection heat transfer Q_{cv}, where:

$$Q_{cv} = \frac{\bar{T}_H - \bar{T}_C}{\sum R} \tag{6}$$

And $\sum R$ is the overall enclosure thermal resistance given by:

$$\sum R = R_{copper} + R_f \tag{7}$$

$$R_{copper} = \frac{\Delta X_{copper}}{A_H\, k_{copper}},\ R_f = \frac{1}{A_H\, \bar{h}} \tag{8}$$

Where, A_H, and ΔX_{copper} are the convection hot surface area of the enclosure and the thickness of the copper plate, respectively. By substituting equations (7) and (8) into (6), the heat transfer through the enclosure is denoted as:

$$Q_{cv} = \left(\bar{T}_H - \bar{T}_C\right) \Big/ \left(\frac{2\Delta X_{copper}}{A_H\, k_{copper}} + \frac{1}{A_H\, \bar{h}}\right) \tag{9}$$

And the average heat transfer coefficient can be obtained as:

$$\bar{h} = 1 \Big/ \left[A_H \left(\frac{\bar{T}_H - \bar{T}_C}{Q_{cv}} - \frac{2\Delta X_{copper}}{A_H\, k_{copper}} \right) \right] \tag{10}$$

The average Nusselt number $\bar{Nu}$ and the modified Rayleigh number Ra^* are denoted as:

$$\bar{Nu} = \bar{h}\, H / k_{nf} \tag{11}$$

$$Ra^* = g\, \beta_{nf}\, Q_{cv}\, H^4 / (A_H \nu_{nf}\ k_{nf}\, \alpha_{nf}) \tag{12}$$

Where, g, β_{nf}, and H are the gravitational acceleration, coefficient of volumetric thermal expansion of nanofluid, and height of the enclosure, respectively. α_{nf}, ν_{nf}, and k_{nf} are the thermal diffusivity, kinematic viscosity, and thermal conductivity of nanofluid, respectively. The viscosity of the nanofluid containing a dilute suspension of small rigid spherical particles has been given by Brinkman [9] as:

$$\mu_{nf} = \frac{\mu_f}{(1-\phi)^{2.5}} \tag{13}$$

The density and thermal diffusivity of the nanofluid at reference temperature is defined as [9]:

$$\rho_{nf} = (1-\phi)\rho_f + \phi\, \rho_p \tag{14}$$

$$\alpha_{nf} = k_{nf} / (\rho C_P)_{nf} \tag{15}$$

The heat capacitance of the nanofluid and part of Boussinesq term as given by Xuan and Roetzel [10] are defined as:

$$(\rho c_p)_{nf} = (1-\phi)(\rho C_p)_f + \phi (\rho C_P)_p \tag{16}$$

$$(\rho \beta)_{nf} = (1-\phi)(\rho \beta)_f + \phi (\rho \beta)_p \tag{17}$$

Here, ϕ is the volume fraction of nanoparticles, and the subscripts f, nf and p

stand for base fluid, nanofluid and particle, respectively. In Equation (15), k_{nf} is the thermal conductivity of the nanofluid, for spherical nanoparticles, is given by Maxwell [11], as:

$$\frac{k_{nf}}{k_f} = \frac{k_p + 2K_f - 2\phi(k_f - k_p)}{k_p + 2K_f + \phi(k_f - k_p)} \quad (18)$$

Where k_p is the thermal conductivity of dispersed nanoparticles and k_f is the thermal conductivity of pure fluid.

5. Results and discussion

Figure (4) shows the relation between average hot surface temperature ($\bar{T}_H$) and average cold surface temperature ($\bar{T}_C$) with time. It is shown from the figure that the steady state conditions were reached at a maximum of 100 min.

Figure (5) indicates the relation between average Nusselt number, $\bar{Nu}$, and the modified Rayleigh number $\overset{*}{Ra}$ for both aspect ratios A=1& 2. It is shown from the figure that the average Nusselt number increases with the increase of the modified Rayleigh number and the increase of aspect ratio.

Figure (6) shows the relation between the average Nusselt number, $\bar{Nu}$, for aspect ratio of 2 and the modified Rayleigh number, $\overset{*}{Ra}$, at nanoparticles volume concentration, ϕ, equal to 0, 0.8 and 2 %. It is shown from the figure that the average Nusselt number increases with the increase of the modified Rayleigh number up to maximum values of about $\overset{*}{Ra} = 10^8$ and then decreases with further increase in $\overset{*}{Ra}$. The figure shows also that the average Nusselt number increases with the nanoparticles volume concentration and takes the highest value at 0.8%.

Figure (7) shows the relation between average hot surface temperature ratio ($\bar{T}_H / T_\infty$) and nanoparticles volume concentration, ϕ, for aspect ratio of 2 and modified Rayleigh number $\overset{*}{Ra}$ equal to 1.94×10^8, 3.37×10^8, 5.21×10^8 and 7.16×10^8. It is shown from the figure that the average hot surface temperature ratio decreases with the increase of nanoparticles volume concentration up to minimum values at ϕ=0.8 % and then increases with further increase in ϕ. The figure shows also that the average hot surface temperature ratio increases with the increase of the modified Rayleigh number.

Figure (8) shows the relation between average Nusselt numbers, $\bar{Nu}$, and nanoparticles volume concentration, ϕ, for modified Rayleigh number, $\overset{*}{Ra}$, equal to 2.48×10^8 and 6.65×10^8. It is shown from the figure that the average Nusselt number increases with the increase of nanoparticles volume concentration up to ϕ=0.8 % and then decreases with further increase in ϕ. This is may be because of increasing the nanoparticles volume concentration intensifies the interaction and collision of nanoparticles. In other words, increasing the concentration of nanoparticles intensifies the mechanisms responsible for reduced heat transfer.

An attempt was made to correlate the experimental data in the following form:

$$\bar{Nu} = 13.245 * ((1 + 0.317\times10^{-9}\times \mathrm{Ra}^* - 0.579\times10^{-18}\times \mathrm{Ra}^{*2}) \times (1 + 0.979\times\phi - 0.354\times\phi^2)) \quad (19)$$

$$0.2\% \le \phi \le 2\%$$

$$10^5 \prec \mathrm{Ra}^* \prec 10^9$$

The calculated average Nusselt number from the above correlation is plotted against the experimental average Nusselt number in Fig.

(9) for aspect ratio 2. The solid line presents the perfect fit whereas the dashed lines present the error band width of $\pm 20\%$.

6. Validation of results

Furthermore, in order to validate the results of the experimental study, Fig. (10) illustrates the relationship between average Nusselt numbers, $\bar{Nu}$, and nanoparticles volume concentration ϕ. The results of Elif [12] are presented for ϕ=0, 0.1, and 0.2 in a rectangular enclosure with heated from bottom wall and cold from top and adiabatic side walls for the enclosure aspect ratio A = 1 and $Ra^{*} = 10^{6}$. It is shown from the figure that average Nusselt number increases with the increase of nanoparticles volume concentration. Two dimensional, steady and incompressible. The thermophysical properties of the nanofluid are assumed to be constant except for the density variation in the buoyancy force. All physical properties of the Titanium Oxide-water nanofluid are evaluated at the ambient temperature. It is clear that, the present study and Elif [12] data tend to have the same trend for average Nusselt numbers with nanoparticles volume concentration.

7. Conclusions

Natural convection in rectangular enclosures filled with TiO_2 - water nanofluid have been studied experimentally, for width-to-height aspect ratios A of 1 and 2 for values of modified Rayleigh number based on the enclosure height in the range $10^{5} \prec \mathrm{Ra}^{*} \prec 10^{9}$. Buoyancy induced flow and heat transfer in a rectangular enclosure under uniform heat flux through the bottom wall, uniform cold temperature through the top wall and insulation side walls have been experimentally investigated. The main results obtained may be summarized as follows:

(1) The average Nusselt number for aspect ratio, A=2, is higher than that for the aspect ratio A= 1;

(2) The hot surface average temperature of decreases with the increase of nanoparticles volume concentration, ϕ, up to minimum values at ϕ = 0.8 % and then increases with further increase in ϕ;

(3) The average hot surface temperature increases with the increase of the modified Rayleigh number;

(4) The heat transfer rate increases with the increase of the modified Rayleigh number up to maximum values at about $Ra^{*} = 10^{8}$ and then decreases with further increase in Ra^{*};

(5) The highest value of the average Nusselt number is located at ϕ = 0.8%;

(6) The average Nusselt numbers increases with the increase of the nanoparticles volume concentration up to ϕ = 0.8 % and then decreases with further increase in ϕ;

(7) A general correlation is obtained to calculate the average heat transfer rate as a function of the modified Rayleigh number Ra^{*} and nanoparticles volume concentration ϕ.

References

1 F.P. Incropera, Convection heat transfer in electronic equipment cooling, J. Heat Transfer, Vol. 110, pp. 1097–1111, 1988.

2 S. Ostrach, Natural convection in enclosures, J. Heat Transfer, Vol. 110, pp. 1175-1190, 1988.

3 S.M. Aminossadati, B. Ghasemi, Natural convection cooling of a localised heat source at the bottom of a nanofluid-filled enclosure, European Journal of Mechanics B/Fluids 28, pp. 630–640, 2009.

4 M. Ali, O. Zeitoun, S. Almotairi, Natural convection heat transfer inside vertical circular enclosure filled with water-based Al_2O_3 nanofluids, Int. J. of Thermal Sciences 63, pp. 115-124, 2013.

5 Incropera, Dewitt, Bergman, Lavine, Fundamentals of heat and mass transfer, sixth ed., p. 929& p. 936.
6 Hsiang- Sheng Huang, Ying-Che Weng, Yu-Wei Chang, Sih-Li Chen, Ming-Tsun Ke, Thermoelectric water-cooling device applied to electronic equipment, Internat. Communications in Heat and Mass Transfer, Vol. 37, pp.140–146, 2010.
7 N. Putra, W. Roetzel, S.K. Das, Natural convection of nano-fluids, Heat Mass Transfer, Vol. 39, pp. 775-784, 2003.
8 E. Abu-Nada, Z. Masoud, A. Hijazi, Natural convection heat transfer enhancement in horizontal concentric annuli using nanofluids, Int. Comm. Heat Mass Transf. Vol. 35 (5), pp. 657-665, 2008.
9 H.C. Brinkman, The viscosity of concentrated suspensions and solutions, J. Chem. Phys. 20, pp. 571–581, 1952.
10 Y. Xuan, W. Roetzel, Conceptions for heat transfer correlation of nanofluids, Int. J. Heat Mass Transfer Vol. 43, pp. 3701–3707, 2000.
11 J. Maxwell, A Treatise on Electricity and Magnetism, Second ed. Oxford University Press, Cambridge, UK, 1904.
12 B. O. Elif, Natural convection of water-based nanofluids in an inclined enclosure with a heat source, International Journal of Thermal Sciences Vol. 48, pp. 2063–2073, 2009.

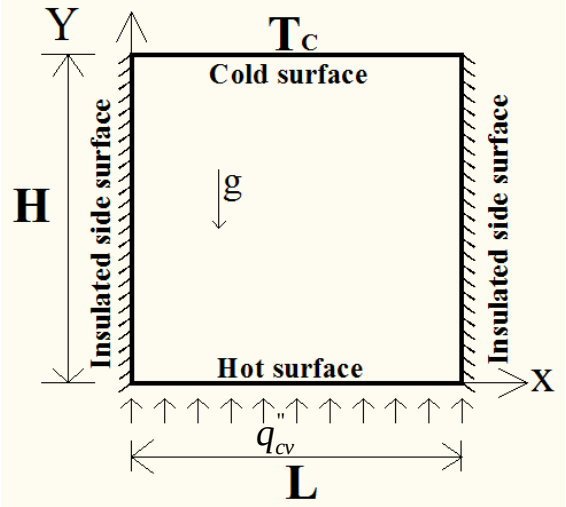

Fig. (1) Test section representation.

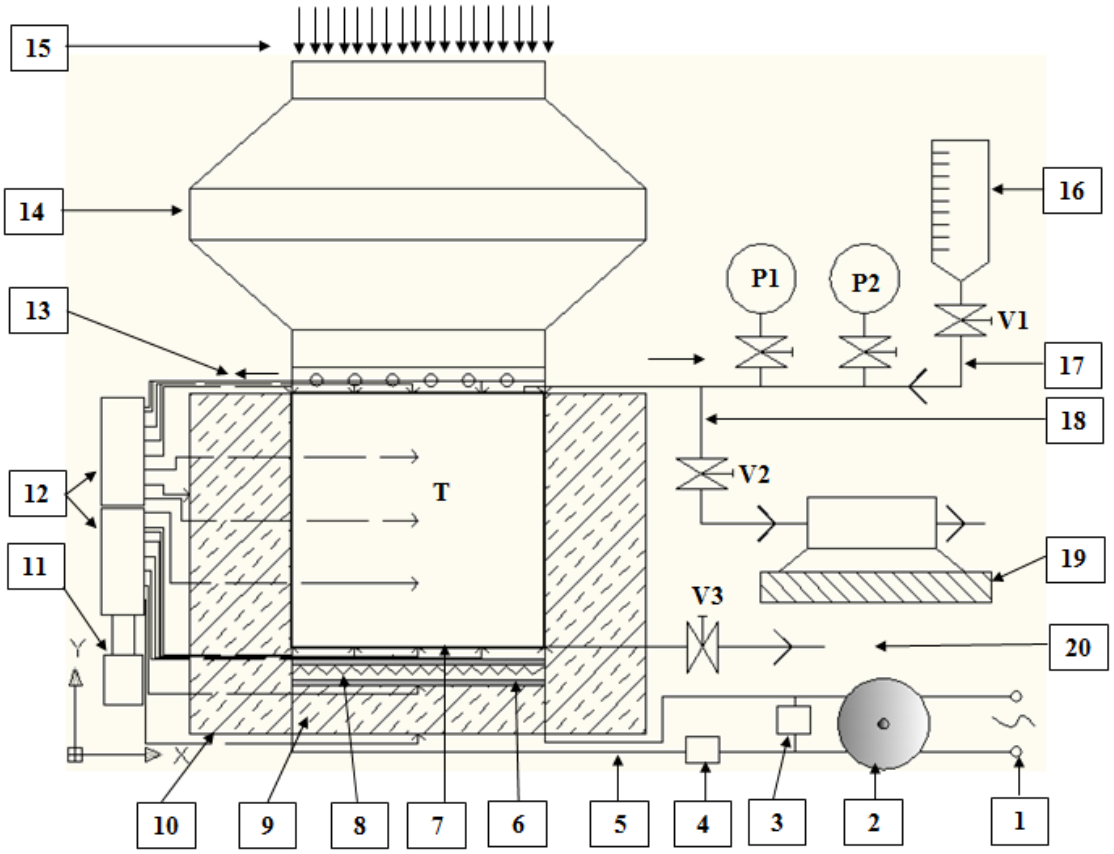

1- Electric power. 5- Electric wire. 9- glass wool. 13- Outlet hot air. 17- Charging pipe line.
2- Variac. 6- Mica Sheet. 10- wood box. 14- Fan. 18- Extracted pipe air line.
3- Voltameter. 7- Enclosure. 11- Computer. 15- Inlet cold air. 19- Vacuum pump.
4- Ameter. 8- Electric heater. 12- Temperature recorder. 16- Tank. 20- Outlet pipe line.
V1- Charging valve. V2- Vacuum valve. V3- Outlet valve. T- Thermocouples (type K)
P1- Vacuum pressure gage. P2- High pressure gage.

Fig. (2) Schematic diagram for the experimental test loop.

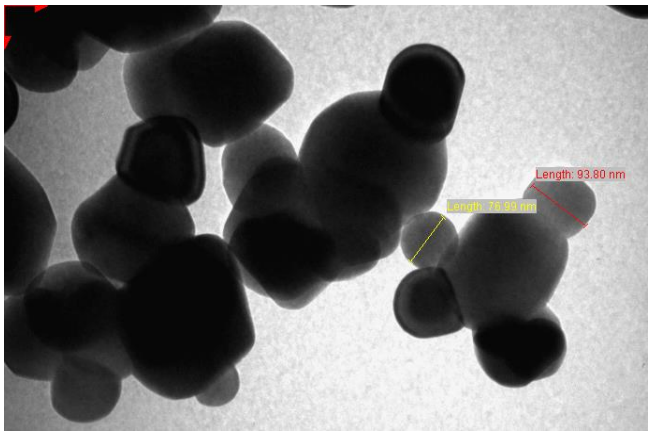

Fig. (3) photograph of nanoparticles shows the agglomeration to bigger sizes.

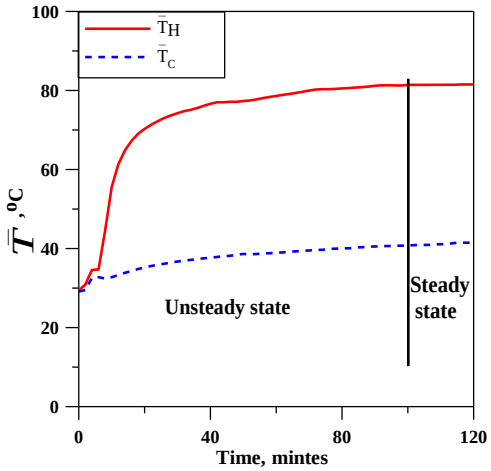

Fig. (4) Samples of temperature variation with time showing the steady state condition.

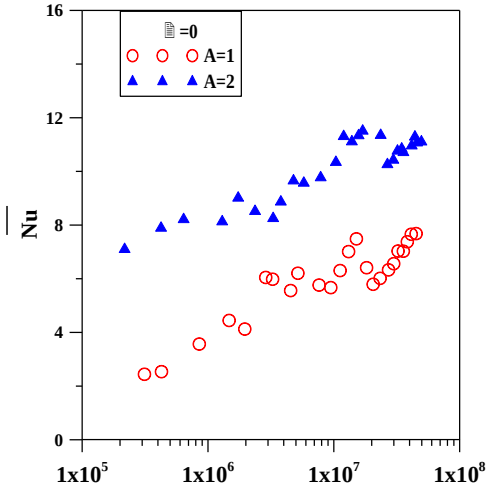

Fig. (5) Effect of A on $\bar{Nu}$ as a function of the modified Rayleigh number.

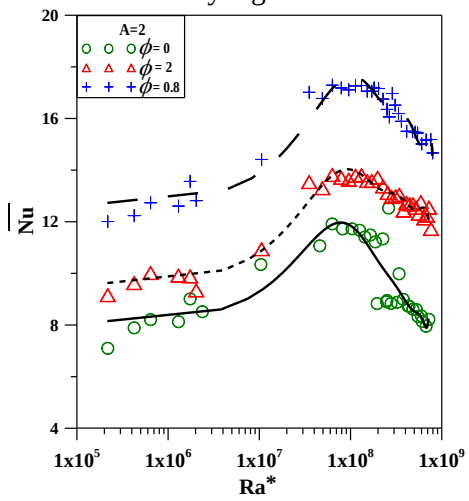

Fig. (6) $\bar{Nu}$ vs. Ra^* for ϕ=0, 0.8 and 2.

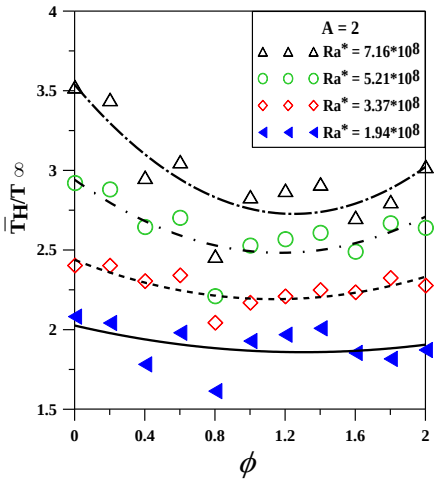

Fig. (7) Effect of ϕ on Average hot surface temperature ratio $\bar{T}_H / T_\infty$ vs. Ra^* for A=2.

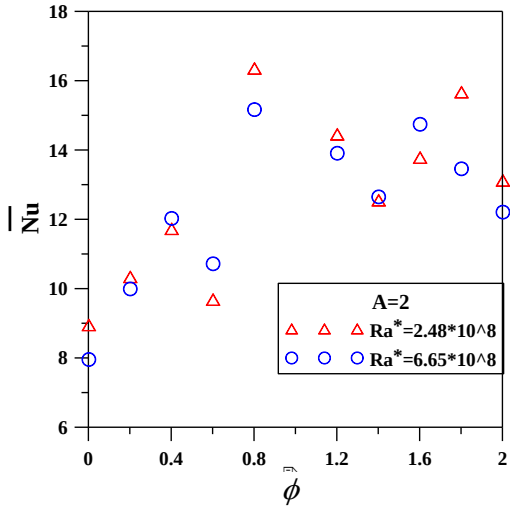

Fig. (8) Effect of ϕ on $\bar{Nu}$ for $Ra^* = 2.48\times10^8$ *and* 6.65×10^8.

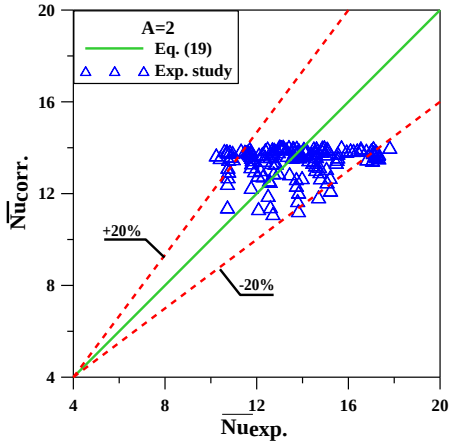

Fig. (9) Correlated average Nusselt numbers versus experimental average Nusselt numbers.

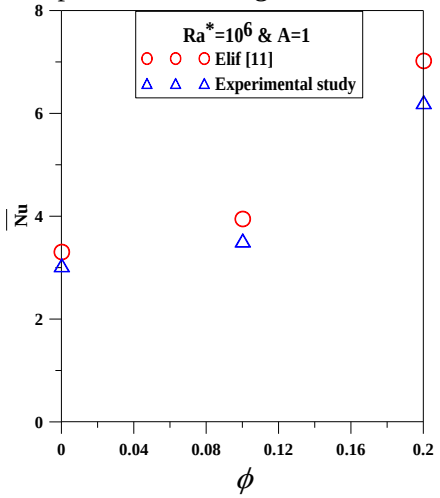

Fig. (10) Comparison between experimental study and Elif [11].